Desalination and Water Treatment
www.deswater.com
doi: 10.1080/19443994.2013.811110

52 (2014) 5900–5911
September

Taylor & Francis
Taylor & Francis Group

Physicochemical characterization and mechanism analysis of native and protonated grapefruit peels adsorbing cadmium

Silke Schiewer[a], Muhammad Iqbal[a,b,*]

[a]*Department of Civil & Environmental Engineering, University of Alaska Fairbanks, PO Box 755900, Fairbanks, AK 99775, USA*
[b]*Centre for Applied Molecular Biology, 87 West Canal Bank Road, Thokar Niaz Baig, Lahore 53700, Pakistan*
Tel. +92 42 35293135; Fax: +92 42 35293148; email: iqbalm@fulbrightmail.org

Received 9 January 2013; Accepted 19 May 2013

ABSTRACT

By-products such as citrus peels are low-cost biosorbents for heavy metal removal from industrial wastewaters. The cadmium-binding mechanism for native and protonated grapefruit peels was investigated. Potentiometric titrations were described well by a two-site model based on carboxyl and hydroxyl sites with pK_a values of 3.9 and 11.1, respectively. A one-site model excellently described increasing metal binding from pH 1 to pH 6 due to decreasing competition with protons. Sorption isotherms showed a maximum Cd^{2+} uptake of 1.7 and 2.2 meq/g for native and protonated peels, respectively. An isotherm model with a 1:2 stoichiometry, where one divalent metal binds to two monoprotic sites, was superior to a 1:1 stoichiometry. For protonated peels, mainly protons were exchanged with Cd^{2+}; for native peels, light metal ions were exchanged. Cd^{2+} sorption was completely reversible by acidic desorption, maintaining the sorption capacity during several cycles. Esterification of carboxyl groups, which reduced Cd^{2+} binding by 80%, showed their importance in metal binding. Formaldehyde treatment to block amine and hydroxyl groups reduced Cd^{2+} binding by a smaller extent. Fourier transform infrared spectra indicated the involvement of carboxyl and hydroxyl groups in metal binding. Grapefruit waste is a promising biosorbent with high capacity and stability.

Keywords: Characterization; Mechanism; Biosorption; Grapefruit peels; FTIR

1. Introduction

Environmental contamination by toxic metals is a serious problem due to their incremental accumulation in the food chain [1,2]. Unlike most organic wastes and the microbial load in aquatic bodies, metal contaminants are not biodegradable, thus becoming a permanent burden on ecosystems [3]. Cadmium competes with Zn in metalloenzymes, inhibiting the normal metabolism [1]. Effects of cadmium poisoning include a reduced sense of smell, reduction of red blood cells, kidney damage, and in extreme cases skeletal deformities and death [1]. The major sources of cadmium release into the environment through wastewater streams are electroplating, smelting, alloy and plastic manufacturing, pigments, battery, fertilizers, mining, and metal refining processes [4]. At present, there are a number of chemical and physical methods for the removal of heavy metals including cadmium

*Corresponding author.

from industrial effluents. However, some of these processes, such as reverse osmosis or ion-exchange resins are cost-prohibitive for the treatment of large wastewater volumes. Others, such as precipitation, which is typically for high metal concentrations, generate toxic sludge and are ineffective, especially when heavy metals are present in wastewater at low concentrations, because no compound is completely insoluble and a residual concentration always remains as expressed by the solubility product [5]. Efficient and environment-friendly technologies, therefore, need to be developed to reduce heavy metal concentration in wastewaters to an acceptable level at affordable costs. This has led to the investigation of alternative low-cost technologies that may be efficiently applied for the removal of heavy metals, particularly at low concentrations (<10 mg/L), where precipitation is not an option.

To this end, biomass from various natural or industrial origins has been investigated for its ability to sequester heavy metals through the process generally known as biosorption [6]. Biosorption uses the ability of various types of biological materials to take up relatively high amount of metal ions by passive sorption and/or complexation [6]. Citrus peels are one such biosorbent material. Citrus is grown in all tropical and subtropical countries and with over 105 million tons annual production and ranks first in total production among fruit crops (http://apps.fao.org). Waste from citrus juice production is dried and sold as a low-value cattle feed at a loss for the processors. In recent years, the potential of lemon [7], orange [8–13], grapefruit [14], and mandarin peels [15] for the binding of pollutants such as cadmium, nitrate, and arsenic has been studied, and suitably high uptake values were found.

To be able to apply biosorbents optimally, the biosorption mechanism needs to be understood. Citrus peels consist mainly of mono-, di-, and polysaccharides. The water-soluble fraction contains glucose, fructose, sucrose, and some xylose, while pectin, cellulose, hemicellulose, and lignin constitute most of the insoluble fraction [16,17]. These polymers contain many carboxyl and hydroxyl groups which can bind heavy metal ions [6]. Titrations of lemon peels modeled by a continuous pK_a spectrum revealed major acidic sites with pK_a values around 4 and 8 [18]. For algal and fungal biosorbents, techniques such as the blocking of binding sites and Fourier transform infrared (FTIR) spectra before and after metal binding have been used. Esterification of carboxyl groups with acidic methanol strongly reduced the Cu^{2+}, Al^{3+}, and Cr^{3+} binding capacity of different algae, indicating the importance of these groups [19,20]. Fourest and Volesky [21] determined by titrations, FTIR, and esterification of carboxyl groups with methanolic hydrochloride and propylene oxide that carboxyl groups were mainly responsible for metal binding by the seaweed *Sargassum*. Similarly, Yun et al. [22] noted for metal-laden seaweed biomass an increase in the carboxyl C=O chelate stretching peak at 1,630 cm^{-1}compared with the free C=O stretching peak at 1,740 cm^{-1}, demonstrating the involvement of carboxyl groups in metal biosorption. Ashkenazy et al. [23] noted that reacting carboxyl groups with propylamine decreased Pb uptake by yeast. In the fungus, *Aspergillus niger*, esterification of carboxyl and methylation of amine groups showed that both sites contribute to metal sorption [24]. To better understand the mechanism of metal biosorption by citrus peels, the goal of this research was therefore to describe metal biosorption by grapefruit peels (GFPs) using a mechanistic model and to investigate the mechanism including identification and quantification of functional groups by potentiometric titration, chemical modification, and FTIR characterization.

2. Materials and methods

2.1. Materials

All chemicals and reagents used were of ACS-reagent grade. Peel waste of grapefruits (*Citrus paradise*) was obtained from the grapefruit juice processing unit of Peace River Citrus Products, Arcadia, Florida, USA. After thorough washing with tap water, the peels were washed three times with nano-pure water (18 Ω resistance) and oven-dried at 50°C until they reached a constant weight. Dried peels were ground and sieved. The peel particles of 0.5–1.0 mm size were used for the adsorption studies.

2.2. Potentiometric titration

GFP was first protonated in order to remove other exchangeable ions present in the raw biomass as described by Schiewer and Volesky [25]: a 0.25 g sample of peels was treated in 250 mL of 0.1 M HCl solution for 6 h in an orbital shaker at 120 rpm and 25°C, and then filtered and washed 3 times with deionized water. Titration can be useful to characterize the pK_a and quantity of functional acid/base groups [26]. Before the titration, the protonated GFP was added to a 250-mL Pyrex beaker containing 50 mL of 0.1 M $NaNO_3$ solution, and the mixture was allowed to stand for 2 h at 25°C for stabilization before the solution was bubbled with nitrogen gas for 2 h with vigorous mixing to remove CO_2 in the solution. The titration was carried

out with an automatic titrator (Metrohm 719 S Titrino) using 0.1 M NaOH solution.

The surface charge S on the peel particle with mass m was calculated according to equation (1) based on the electro-neutrality equation of the solution with volume V [27]:

$$S = ([OH^-] + [NO_3^-] - [H^+] - [Na^+])V/m \text{ (meq/g)} \quad (1)$$

$[Na^+]$, $[NO_3^-]$, $[H^+]$ and $[OH^-]$ are the concentrations of sodium, nitrate, protons, and hydroxyl (mol/L), respectively, in the solution. Since NO_3^- and Na^+ from the background electrolyte (0.1 M $NaNO_3$) cancel each other's charge out, only the equivalents of NO_3^- from acid addition and Na^+ from base addition have to be considered in addition to OH^- and H^+ from pH measurements.

2.3. Adsorption studies

In order to determine the adsorption capacity of GFP, 50 mg samples of GFP was added to 50 mL of metal solution of known concentrations (0.178–10.67 meq/L, i.e. 10–600 mg/L) in 250-mL Erlenmeyer flasks that had been prewashed with 1% HNO_3 solution. The flasks were shaken on an orbital shaker at 120 rpm and 25 ± 2˚C for 180 min, until equilibrium was reached, followed by filtration through Whatman No. 40 filter paper. The Cd^{2+} concentration in the filtrate was determined by atomic absorption spectrophotometer (AAnalyst 300, Perkin-Elmer, Waltham, MA, 02451 USA). Resulting final concentrations ranged between 0.2 and 500 mg/L, spanning several orders of magnitude.

To evaluate the effect of pH on the adsorption of Cd^{2+}, adsorption experiments as described above were performed at different fixed pH values. About 50 mg samples of GFP was added to 50 mL of 1.78 meq/L Cd^{2+}solution in 250-mL Erlenmeyer flasks. The resulting suspension was agitated for 180 min on a magnetic stirrer at 150 rpm. The pH value was maintained at 2, 3, 4, 5, and 6 by incrementally adding 0.1 M HCl or 0.1 M NaOH. The pH of the adsorption mixture was continuously monitored using an immersed pH electrode connected to a pH meter (Model 8015, VWR Scientific) throughout the adsorption experiments.

All sorption experiments were conducted in triplicate, and the mean values were reported. The mean deviations between the triplicates were always less than 5%. Standard deviations were in average 0.02 meq/g, which rendered error bars difficult to distinguish from the data markers.

The metal uptake per gram of biosorbent material was determined using the mass balance. If C_0 and C_e are the initial and final metal concentrations (mg/L or meq/L), respectively, V is the suspension volume (L) and m is the mass of biosorbent material (g), then the equilibrium metal uptake q (mg/g or meq/g) can be calculated from the experimental data as [6]:

$$q = \frac{V(C_0 - C_e)}{m} \quad (2)$$

2.4. Adsorption/desorption cycles

The adsorption step was performed using 50 mL of Cd solution with an initial concentration of 25 mg/L at pH 5.0 and 50 mg of native or protonated peels. For desorption of the adsorbed metal ions from the metal loaded GFP, 50 mg of metal loaded adsorbent was added to a 250-mL Erlenmeyer flask containing 50 mL of desorbing agent (0.1 M HCl) and shaken at 100 rpm on an orbital shaker at 25 ± 2˚C. After 2 h shaking, the solution was centrifuged and supernatant was analyzed for metal ions desorbed. Acidic desorption was chosen since it does not introduce other ions such as Ca^{2+} which could compete with the target metal for binding sites. Treatment with 0.1 M HCl did not damage the sorbent. Desorption of with 0.1 M acid is common since it is typically fast and effective for displacing metals from acidic groups and the sorbent can be reused [28,29].

2.5. Modeling error analysis

In order to evaluate the error of the model predictions, the root mean square errors (RMSE) were calculated. The sum of the square of the difference between metal removal experimental data (q), and model predictions (q_m) was divided by the number of data points (p) for each data set and the square root of this term was taken.

$$\text{RMSE} = \sqrt{\frac{\sum_1^p (q - q_m)^2}{p}} \quad (3)$$

2.6. Elemental composition

For the determination of Ca, Mg, K, Na, Fe, and Mn, both native- and Cd(II)-laden GFP were processed by Association of Analytical Communities dry ashing method [30], and the resulting filtrate was analyzed on AAS.

2.7. Chemical modification of GFP

Modification of GFP carboxyl groups with acidic methanol was performed according to the method of Gardea-Torresdey et al. [19]. Ten grams of GFP (0.5–1 mm) was suspended in 650 mL of anhydrous methanol and 5.4 mL of concentrated HCl. The reaction mixture was shaken on a rotary shaker for 48 h at 100 rpm. The reaction was stopped by the addition of a large volume of cold nanopure water, and resultant peels were separated by centrifugation. This treated peel was then washed repeatedly with nanopure water to remove excess HCl and CH_3OH, freeze-dried and stored in sealed glass bottles for subsequent experiments.

Carboxyl-free GFP was prepared in aqueous propylene oxide solution according to the procedure described by Fourest and Volesky [21]. Protonated GFP biomass was allowed to stand in 37% (w/w) propylene oxide solution (20 mL/g) at room temperature for 48 h. To stop the reaction, the excess propylene oxide was removed by repeated washing with nanopure water. The treated GFP was then freeze-dried and stored for subsequent experiments.

Methylation of hydroxyl group of GFP biomass was carried out according to the method of Kapoor and Viraraghavan [24]. One gram of biomass was contacted with 20 mL of formaldehyde (HCHO) and 40 mL of formic acid (HCOOH), and the reaction mixture was shaken on rotary shaker for 6 h at 125 rpm. To stop the reaction, the GFP biomass was separated by centrifugation and thoroughly washed with nanopure water and freeze-dried. The aim of chemical modification was to investigate the role of functional groups (carboxyl and hydroxyl) of GFP in the biosorption of metals ions and to elucidate the mechanisms of metal removal.

2.8. FTIR spectroscopy

FTIR spectroscopy was used to determine the changes in vibration frequency in the functional groups in the protonated GFP, Cd^{2+}-loaded GFP and GFP after Cd^{2+} binding and subsequent desorption. The spectra were collected by a Thermo Nicolet IR-100 Spectrometer (Thermo Nicole Corporation, Madison, USA) within the wave number range of 400–4,000 cm^{-1}. All three specimens were first ground in a Wig L Bug Grinder (Crescent Dental MFG. CO. Chicago, ILL, USA) and then mixed with fine KBr powder at an approximate ratio of 1:100 for the preparation of pellets (100 mg) and pressed into a thin film, used for recording the spectra. All samples were scanned three times, with no significant difference between the spectra. The background obtained from the scan of pure KBr was automatically subtracted from the sample spectra. All spectra were plotted using the same scale on the absorbance axis.

3. Results and discussion

3.1. Potentiometric titration

As shown in Fig. 1, the negative surface charge of protonated GFPs increased rapidly between pH 3 and 5, changed only slightly between pH 5 and 10, and increased again rapidly beyond pH 10. This indicates the presence of a major acidic site with pK_a around 4 and a further site with $pK_a > 10$. It should be noted that these are apparent pK_a values, which (unlike the number of sites) can vary with the ionic strength [26]. Intrinsic pK_a values can be determined by titrations at different ionic strengths, which is necessary when employing a model that includes electrostatic effects [26].

Since GFPs contain about 20% of pectin [17,31], which features many carboxyl groups, the first site, with pK_a around 4, corresponds to carboxyl groups of pectin. The second site appears to be hydroxyl groups, which occur in large numbers in pectin and cellulose and are known to have pK_a values around 10 [32].

To quantify the pK_a and site quantity of the two types of sites, a two site model was fitted to the data. For a binding site B_j with dissociation constant K_{aj}, the following equations apply:

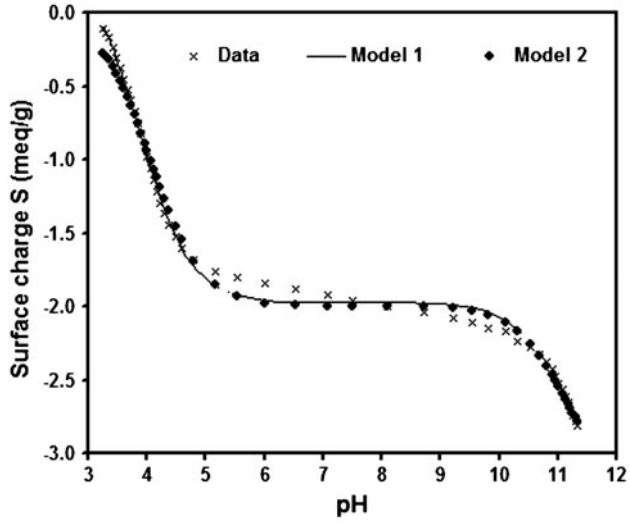

Fig. 1. Potentiometric titration of protonated GFPs at 0.1 M $NaNO_3$ background electrolyte. Data and model predictions. Model 1: two types of acidic sites and initial charge. Model 2: two types of acidic sites without initial charge.

Table 1
Site quantities and pK_a values determined from potentiometric titration of protonated GFPs, obtained by fitting a two-site model without or with initial charge

B_0 (meq/g)	B_{T1} (meq/g)	pK_{a1}	B_{T2} (meq/g)	pK_{a2}	RMSE
0	2.00	4.06	1.30	11.15	0.075
0.36	2.33	3.87	1.23	11.06	0.048

$$[BH_j] \rightarrow [H^+] + [B_j^-] \quad (4)$$

$$K_{aj} = [H^+][B_j^-]/[BH_j] \quad (5)$$

$$[B_{Tj}] = [B_j^-] + [BH_j] \quad (6)$$

The total site concentration (B_{Tj}) consists of the free binding site concentration (B_j^-) and the protonated binding site concentration (BH_j) (mol/L). The charge can be calculated by combining Eqs. (5) and (6) for two sites B_1 and B_2:

$$S_{\text{mod}} = S_o + \frac{B_{T1}}{1 + [H^+]/K_{a1}} + \frac{B_{T2}}{1 + [H^+]/K_{a2}} \quad (7)$$

The term S_o is added in order to account for any initial charge on the surface. Table 1 shows the parameters optimized by nonlinear fitting, minimizing the RMSE.

The quantity of the first acidic site was 2.0 meq/g if the initial surface charge S_o was assumed to be zero. If an initial surface charge S_o was taken into consideration, its optimal value was +0.36 meq/g, which increased the quantity of the first site to 2.33 meq/g. pK_a values were similar in both cases, around 4 for the first and 11 for the second site. When the initial charge was taken into account, the model fit below pH 5 improved, resulting in overall lower RMSE values. As shown below, the site quantity of 2.33 meq/g corresponded well to the maximum metal-binding capacity.

3.2. Effect of pH on metal binding

Fig. 2 shows the effect of pH on metal binding. The maximum metal binding achieved for protonated peels was higher than that for native peels. As typical for the biosorption of cations by many biosorbents, sorption increases with pH up to a maximum value. This effect is due to the competition of metal ions and protons for the same binding sites, whereby protons reduce metal binding at low pH values [25].

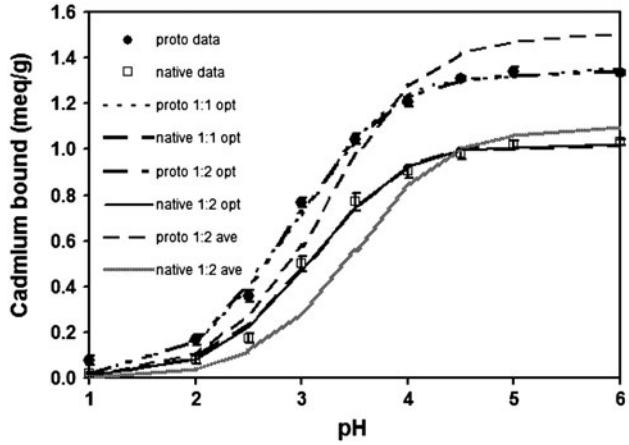

Fig. 2. Effect of pH on Cd^{2+} uptake by protonated and native GFPs for an initial Cd^{2+} concentration 100 mg/L and a sorbent dosage of 1 g/L. Data (mean of triplicates, error bars indicate standard deviation) and predictions of the following model versions: 1:1 stoichiometry with optimized parameters, 1:2 stoichiometry with optimized parameters, 1:2 stoichiometry with C_t and pK_a from titration and average K_M.

To describe the interactions of metal ions and protons with binding sites, one can either assume that each metal ion M binds to one binding site B or to two binding sites. For a 1:1 stoichiometry, the following equations apply [33]:

$$M + B^- \rightarrow BM \quad (8)$$

$$K_M = \frac{BM}{B^- C_e} \text{ (L/mmol)} \quad (9)$$

$$B_T = B^- + BH + BM \text{ (meq/g)} \quad (10)$$

$$q = BM = \frac{B_T K_M C_e}{1 + [H^+]/K_a + K_M C_e} \text{ (meq/g)} \quad (11)$$

If on the other hand, each divalent metal ion binds to two monoprotic sites, the following equations proposed by Schiewer and Volesky [25] apply:

$$M^{2+} + 2B^- \rightarrow 2BM_{0.5} \quad (12)$$

$$K_M = \left(\frac{BM_{0.5}}{B^- C_e}\right)^2 \text{ (L/mmol)} \quad (13)$$

$$B_T = B^- + BH + BM_{0.5} \text{ (meq/g)} \quad (14)$$

$$Q = \mathrm{BM}_{0.5} = \frac{B_T (K_M C_e)^{0.5}}{1 + [H^+]/K_a + (K_M C_e)^{0.5}} \ (\mathrm{meq/g}) \qquad (15)$$

For the pH range 1–6, only the carboxyl groups with pK_a around 4 were considered in the modeling. At these pH values, hydroxyl groups with pK_a around 11 would remain protonated and are therefore not expected to contribute to metal binding. The model parameters B_T, K_M, and pK_a were optimized for both stoichiometries by minimizing the RMSE. The resulting values are listed in the top half of Table 2.

If all three parameters were optimized to fit the data of Fig. 2 ("all opti"), the model fit using Eqs. (11) and (15) was excellent. For either sorbent and stoichiometry, RMSE values were around 0.03 meq/g, which corresponds to about 1 % of the maximum capacity. The curves for both stoichiometries virtually coincided, i.e. either model can be used successfully if the metal concentration is not varied. The excellent fit of a one site model gives a first indication that in the studied pH range only the first binding site with pK_a around 4 contributes to metal binding.

For the protonated peels, the site quantities B_T (2.37, 1.73) and pK_a values (3.79, 3.80) were similar to those obtained by titration ($B_T = 2.33$, pK_a 3.87 from Table 1). For the native biomass, the pK_a values were a little lower (pK_a 3.56, 3.79), which can be explained by the presence of other ions (Ca^{2+}, Mg^{2+}, K^+, Na^+, see Section 3.5). Even though the titrations were performed at a background electrolyte concentration of 0.1 M, the additional ions originally present in the native biomass could have lowered the apparent pK_a value. Electrostatic attraction of other cations to the vicinity of acidic binding sites can lower the concentration of protons at the solid/liquid interface. Thus, a higher proton concentration in the bulk solution is necessary to achieve the same level of protonation, which corresponds to a lower pK_a value. For carboxyl groups in an algal biosorbent, the apparent pK_a value dropped from almost 5 to about 3 with increasing ionic strength [26].

Ideally, the same site concentration and pK_a as determined in titrations should apply for modeling the metal binding. Therefore, Table 2 and Fig. 2 also show model predictions for which only the metal binding constant was optimized to fit the data of Fig. 2. As expected, the RMSE are higher than for optimized pK_a and B_T; however, model predictions were still very good with RMSE of 0.11 or lower. It should be noted that even though the native peels had a lower maximum Cd^{2+} binding than protonated peels (Fig. 2), the data could be modeled using the same B_T value as for protonated peels. For the chosen initial concentration of 100 mg/L, not all sites were saturated with Cd^{2+}, but some sites were still occupied with protons (at lower pH) or occurred as free negatively charged groups (at pH 4 or higher). Therefore, the highest values shown in Fig. 2 do not represent the maximum sorption capacity determined in isotherm studies.

3.3. Metal-binding isotherms

Metal-binding isotherms for native and protonated biomass are shown in Fig. 3. A plateau was reached for equilibrium Cd^{2+} concentrations above 150 mg/L with maximum binding capacities of 1.7 meq/g for native and 2.2 meq/g for protonated peels. The latter value is very close to the determined carboxyl site quantity of 2.33 meq/g, giving a further indication that Cd^{2+} may be bound to carboxyl groups. The observed binding capacity was considerably higher than that determined by Schiewer and Patil [18], where unprocessed GFPs had a capacity of 0.49 meq/g compared with 0.93 meq/g for lemon peels. Protonated peels with maximum experimental Cd^{2+} binding of 2.24 meq/g (a conservative number, since the extrapolated q_{max} or B_t typically exceeds the maximum experimental uptake) would fall in the top 10% of 180 biosorbents whose q_{max} values were compared in a review by Lodeiro et al. [34], about half of which had capacities of 1 meq/g or less. Most of the sorbents with higher uptake were algae, which are not available as a byproduct but would have to be harvested, which involves additional cost. Furthermore, it is not clear for some of the top sorbents if experimental uptake came close to the extrapolated q_{max} values. This demonstrates that the actual grapefruit waste used here is a promising sorbent, obtained at minimal cost with very little sorbent processing, and ranking among the highest biosorbents for Cd^{2+}uptake as summarized in [35].

Especially, protonated peels showed a very high affinity for Cd^{2+}, whereby half of the maximum capacity was already reached at an equilibrium concentration of about 10 mg/L. This indicates that the sorbent can be used effectively for treating solutions with low metal concentrations.

To model the isotherms using Eqs. (11) and (15), the parameters B_T, pK_a, and K_M were optimized for the data of Fig. 3. Results are shown in Fig. 3 and the bottom half of Table 2. Obviously, fits were best if all three parameters were optimized to fit the data of Fig. 3; however, good fits were still achieved when the B_T and pK_a values determined in titrations were used and only K_M was optimized. As a further model

Table 2
Parameters for models with 1:1 and 1:2 stoichiometries for describing pH effects and isotherms of Cd^{2+} binding to native or protonated GFPs. The site quantity B_T and pK_a value were either optimized for the respective data set or used as determined from the titration curves (Table 1). K_M was either optimized or the average optimum value for pH effects and isotherms was used

			Native				Protonated			
			B_T (meq/g)	pK_a	K_M (L/meq)	RMSE (meq/g)	B_T (meq/g)	pK_a	K_M (L/meq)	RMSE (meq/g)
pH effect	1:1 stoich	All opti	3.44	3.56	0.010	0.031	2.37	3.79	0.055	0.036
		Opti K_M	2.33[a]	3.87[a]	0.022	0.075	2.33[a]	3.87[a]	0.061	0.046
		Ave K_M	2.33[a]	3.87[a]	0.017[b]	0.125	2.33[a]	3.87[a]	0.077[b]	0.109
	1:2 stoich	All opti	3.09	3.42	0.006	0.025	1.73	3.80	0.495	0.029
		Opti K_M	2.33[a]	3.87[a]	0.023	0.105	2.33[a]	3.87[a]	0.121	0.111
		Ave K_M	2.33[a]	3.87[a]	0.019[b]	0.110	2.33[a]	3.87[a]	0.140[b]	0.115
Isotherm	1:1 stoich	All opti	1.80	4.05	0.038	0.033	2.14	4.06	0.183	0.176
		Opti K_M	2.33[a]	3.87[a]	0.012	0.200	2.33[a]	3.87[a]	0.092	0.206
		Ave K_M	2.33[a]	3.87[a]	0.017[b]	0.226	2.33[a]	3.87[a]	0.077[b]	0.208
	1:2 stoich	All opti	2.80	4.37	0.010	0.076	2.73	3.98	0.061	0.050
		Opti K_M	2.33[a]	3.87[a]	0.016	0.102	2.33[a]	3.87[a]	0.158	0.138
		Ave K_M	2.33[a]	3.87[a]	0.019[b]	0.110	2.33[a]	3.87[a]	0.140[b]	0.140
Average opti 1:1			2.62	3.80	0.024	0.032	2.26	3.93	0.119	0.106
Average opti 1:2			2.94	3.89	0.008	0.051	2.23	3.89	0.278	0.040

[a]Values determined in titration.
[b]Same average K_M value used to model pH effects and isotherm.

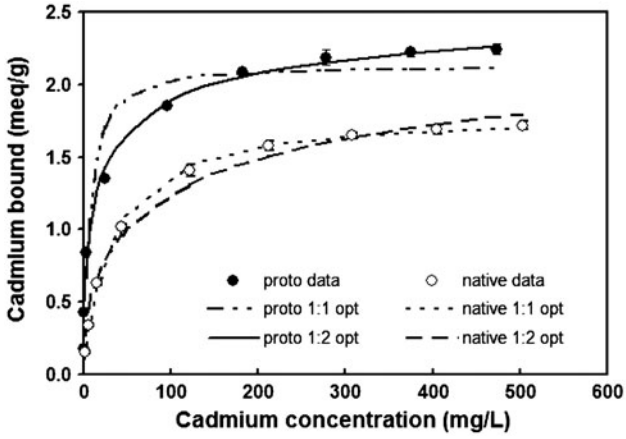

Fig. 3. Sorption isotherms for Cd^{2+} binding by protonated and native GFPs at pH 5.0. Data (mean of triplicates, error bars indicate standard deviation) and predictions of the following model versions: 1:1 stoichiometry with optimized parameters, 1:2 stoichiometry with optimized parameters.

variation, the same average metal-binding constant was used to model the pH effect and the isotherms. As shown by the dashed lines in Fig. 2 and the model in Fig. 4(a) and (b), reasonably good fits were still obtained if the same average metal binding constant was used to model both sets of data.

For the native biomass, both models had excellent predictions with RMSE as low as 1–3% of B_T. For the protonated biomass, the 1:2 stoichiometry (solid lines in Fig. 3) was superior to the 1:1 stoichiometry (dotted lines in Fig. 3). It makes sense from a mechanistic point of view that a divalent ion binds to two monoprotic sites as assumed by the 1:2 stoichiometry. One of the known pectin gelation mechanisms is the bridging of divalent cations between two polymer chains by binding to functional groups on each polymer.

3.4. Release of protons during metal binding

Upon addition of sorbent to the metal solution at pH 5, the pH dropped rapidly. The resulting pH before addition of any NaOH for pH adjustment is shown on the second *y*-axis of Fig. 4. The pH dropped for native peels from 4.7 to 3.9 and for protonated peels from 3.8 to 2.9. Due to the logarithmic nature of the pH value, the actual amount of protons released was higher for protonated peels than for native peels. The proton release was calculated from the amount of NaOH added for pH adjustment and plotted on the primary y axis for comparison with the amount of metal bound.

It can be observed that for protonated biomass (Fig. 4(a)), metal binding was accompanied by proton

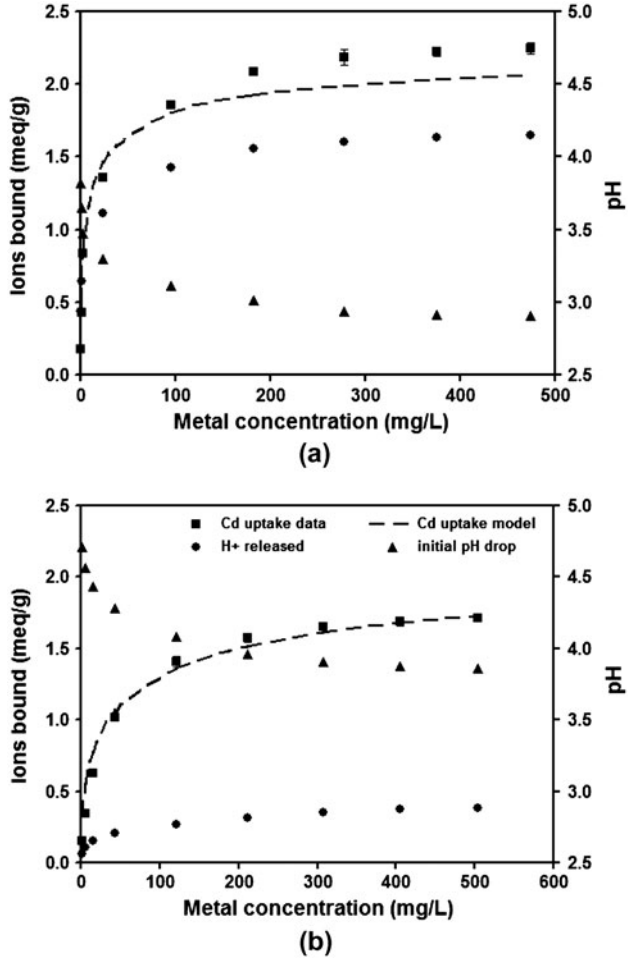

Fig. 4. Initial pH drop and release of protons during binding of Cd^{2+} at pH 5.0 by (a) protonated and (b) native GFPs. Model prediction for Cd^{2+} binding according to 1:2 stoichiometry with C_t and pK_a from titration and average $K_{M.}$

release of almost equal magnitude. This means ion exchange between Cd^{2+} ions and H^+ ions played a major role. Minor amounts of other ions such as Ca^{2+}, which may have remained bound after protonation could be responsible for the difference between metal binding and proton release. For native biomass on the other hand (Fig. 4(b)), proton release was very low since most sites were occupied by other ions, such as Ca^{2+}, Mg^{2+}, K^+, Na^+, as discussed in Section 3.5. Therefore, ion exchange with those ions was more important.

Due to the presence of those competing ions, the maximum metal binding by native biomass (1.7 meq/g) was lower than that of protonated biomass (2.2 meq/g). Nevertheless, the metal uptake could be modeled for both materials using a site quantity of 2.33 meq/g as determined in the titration

Table 3
Ionic composition (meq/g) of native peels as determined by digestion, ions remaining after sorption of Cd^{2+}, and ions released during Cd^{2+} sorption at pH 5 for an initial concentration of 600 mg/L

	Ca	Mg	K	Na	Mn	Fe	Sum
Digestion	0.87	0.39	0.14	0.10	0.0003	0.0037	1.51
Remaining after sorption	0.05	0.03	0.00	0.03	0.0002	0.0008	0.12
Release during sorption	0.83	0.36	0.14	0.06	0.0001	0.0029	1.39
% released	95	92	97	65	29	80	92

of protonated biomass (Fig. 1, Table 1). Even when the same average metal-binding constant was used for modeling pH effects and isotherms, leading to larger RMSE than for optimized parameters (Table 2), the model predictions were good as shown in Fig. 4.

3.5. Ionic composition of native peels and ion release during metal binding

The amount of ions originally present on native peels was determined by digestion. As shown in Table 3, the major ions were Ca^{2+} and Mg^{2+}, followed by K^+ and Na^+, with negligible quantities of Mn and Fe. During Cd^{2+} sorption with an initial concentration of 600 mg/L, to achieve site saturation, 92% of the originally present ions were released.

If the amount of protons released (calculated from NaOH added) is added to the sum of other ions released, a total of 1.78 meq/g is obtained, which matches perfectly with the amount of Cd^{2+} bound (1.75 meq/g), showing that ion exchange is prevalent also for native peels. Fig. 5 shows the amount of ions present initially (including H^+), ions released during Cd^{2+} sorption, and ions bound after the sorption equilibrium is reached (including Cd^{2+}), illustrating that the total amount of ions bound remains constant during this ion-exchange process.

3.6. Adsorption/desorption cycles

When the same sorbent material was exposed to five consecutive adsorption/desorption cycles, adsorption remained very high with metal removal efficiencies of more than 90%, except during the first cycle for native biomass where metal removal was only 77% (data not shown). Complete desorption was achieved with efficiencies of 98–99% (data not shown). As depicted in Fig. 6, the amount of metal bound remained almost constant during five adsorption/desorption cycles, decreasing by less than five percent. This indicates complete regeneration of the sorbent with good chemical and mechanical stability; the desorption treatment did not damage the sorbent. The reversibility of the sorption process is consistent with the above mentioned ion exchange between heavy metal ions and protons (Fig. 4).

For native peels, there was even an increase in the sorption capacity from the first to the second cycle, in conjunction with an increase in metal removal from 77 to 96%. This can be explained based on Figs. 3–5. Native biomass generally showed lower metal binding than protonated biomass (Fig. 3), due to competition by other ions such as Ca^{2+} and Mg^{2+} initially present in the biomass (Fig. 5). During the first adsorption step, most of these other ions are released from the sorbent (Fig. 5). During desorption, protons replace Cd^{2+} and any remaining other cations. Therefore, these ions no longer interfere with metal binding during subsequent cycles and the native biomass essentially behaves like protonated biomass.

3.7. Identification of binding sites by chemical modification of functional groups

Since metal binding could be described with a one-site model based on acidic groups with pK_a around 4, it is highly plausible that carboxyl groups

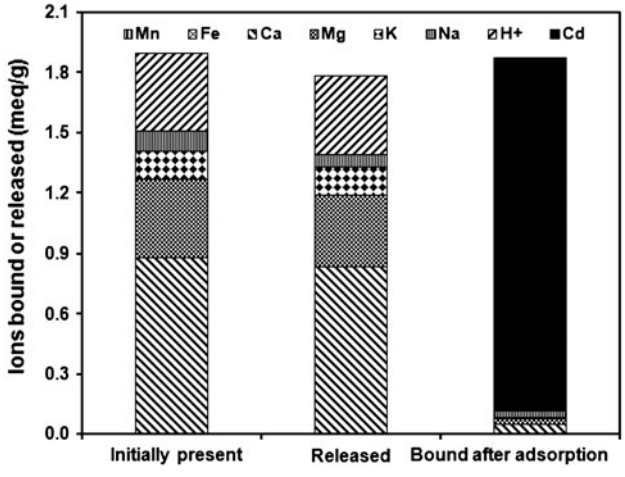

Fig. 5. Ions bound to native GFPs, ions released during binding of Cd^{2+} and ions bound to peels after Cd^{2+} adsorption for an initial Cd^{2+} concentration 600 mg/L, pH 5.

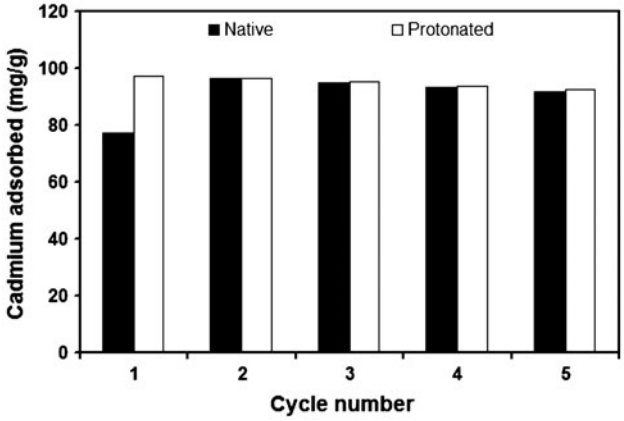

Fig. 6. Cd^{2+} binding at pH 5.0 for GFPs after several cycles of adsorption with 25 mg/L initial Cd^{2+} concentration and desorption with 0.1 M HCl.

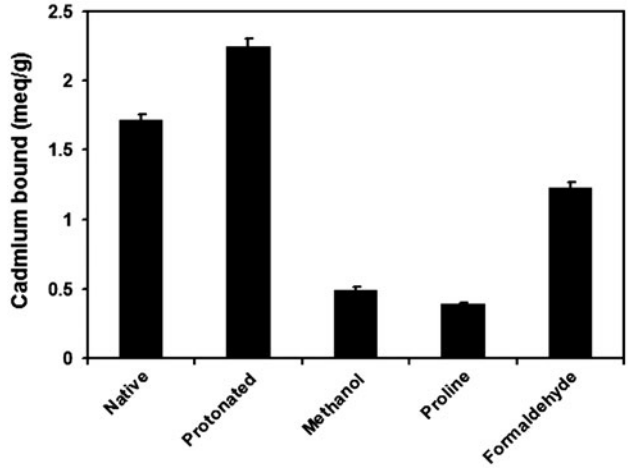

Fig. 7. Cd^{2+}-binding capacity at pH 5.0 for GFPs after different treatments, for an initial Cd^{2+} concentration of 600 mg/L. Acidic methanol and proline treatments were used to block carboxyl groups, formaldehyde treatment to block amine and hydroxyl groups.

play a dominant role in the binding of Cd^{2+} by GFPs. To confirm this hypothesis, carboxyl groups were esterified and the metal-binding capacity after modification was determined and compared with native or protonated peels. Since all three treatments occur under acidic conditions, their effect is best compared with protonated biomass. Fig. 7 shows that the metal-binding capacity for an initial Cd^{2+} concentration of 600 mg/L drops by about 80% when carboxyl groups are blocked by esterification with acidic methanol or propylene oxide. This indicates that carboxyl groups are responsible for most of the metal binding.

Formaldehyde treatment, which blocks amine and hydroxyl groups [20] reduced metal binding by 50% compared to protonated or 30% compared with native biomass. Those groups may therefore also play a role in Cd^{2+} binding. The remaining binding after formaldehyde treatment is due to carboxyl groups. It is possible that the positive charge of amine groups was responsible for the positive base charge (Table 1).

3.8. Investigation of binding sites using FTIR

To further confirm the important role of carboxyl groups in Cd^{2+} binding by GFPs, FTIR spectra were obtained for protonated peels, protonated peels after binding of Cd^{2+}, and the same peels after Cd^{2+} was subsequently desorbed. The spectra depicted in Fig. 8 show the typical hydroxyl (–OH) peak at wave number 3,424–3,431 cm^{-1}, alkyl ($-CH_n$) peak at wave number 2,927 cm^{-1}, peak "1" at wave number 1,741 for the C=O bond of carboxyl groups and their esters, and peak "2" at wave number 1,625 to 1,638 cm^{-1} for asymmetric stretching of the carboxylic C=O double bond. After adsorption of Cd^{2+}, peak "1" stayed in position but decreased in size, whereas peak "2" increased significantly in size and shifted very strongly, moving to 1,625 cm^{-1}. This clearly shows the involvement of carboxyl groups in Cd^{2+} binding. For seaweeds and their component alginic acid, the peak around 1,630 cm^{-1} was similarly attributed to metal chelates of carboxyl groups [21,22,36,37]. A smaller shift was observed for OH groups whose peak shifted from 3,431 to 3,424 cm^{-1}, indicating that OH groups participate in metal binding. It is interesting to note that after desorption of Cd^{2+} by acid, the spectra essentially shifted back to their original position. This confirms that the adsorption process is reversible and any change of spectrum during Cd^{2+} binding was indeed due only to Cd^{2+} binding and not to other effects.

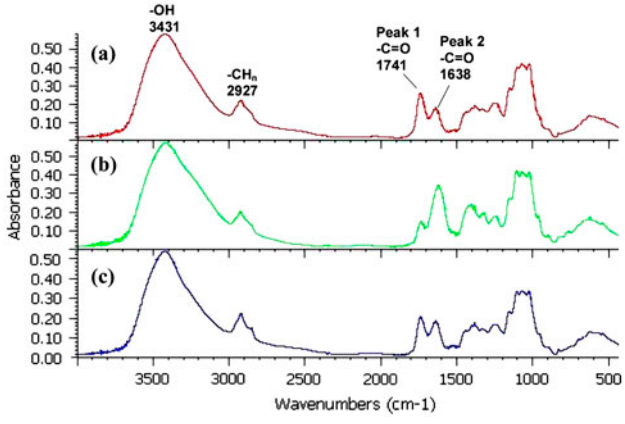

Fig. 8. FTIR spectra of (a) protonated GFPs, (b) protonated peels after adsorption of Cd^{2+}, and (c) protonated peels after Cd^{2+} adsorption and subsequent desorption.

In the literature, different groups were identified as being involved in metal binding by plant-based biosorbents. For base-treated juniper fibers, carboxyl groups were identified as the main binding site for Cd^{2+} binding according to FTIR [38]. FTIR spectra of grape stalks indicated that the lignin C–O bond may be involved in Cu binding [39]. Copper ions affected the bands for C=C vibrations of carbon rings in dried leaves [40]. For Pb^{2+} binding by pectin, a significant shift for the carboxylate peak around 1,630 cm^{-1} was observed, similarly as in the present work, and an additional peak at 1,384 cm^{-1} appeared upon Pb^{2+} binding [27], which was not observed in the current study.

4. Concluding remarks

Potentiometric titrations revealed two main acidic sites with pK_a values around 4 and 11, which are carboxyl and hydroxyl groups, respectively. The titration curve was predicted well by a two site model with a small initial positive charge.

Metal binding increased with pH due to decreasing competition by protons. This effect could be modeled very well with a one site model, using the pK_a value and site quantity determined in titrations.

Metal binding by protonated peels was higher than by native peels, where naturally present cations may have competed with cadmium for the same binding sites. The maximum capacity, reached at Cd^{2+} concentration in solution above 150 mg/L, was 1.7 meq/g for native and 2.2 meq/g for protonated peels. This means GFPs rank in the top tier of biosorbents for cadmium uptake.

Cd^{2+} sorption isotherms were better described by a model assuming that divalent cations bind to two monoprotic sites, compared with the more commonly assumed 1:1 stoichiometry, on which for example the Langmuir model is based.

Ion exchange occurred during metal binding: for native peels, the amount of ions such as Ca^{2+} released was equal to the amount of cadmium bound; for protonated peels, protons were exchanged against Cd^{2+}.

Cd^{2+} sorption was completely reversible by acidic desorption, and the sorption capacity was maintained during several adsorption/desorption cycles. For native peels, the binding capacity even increased from the first to the second cycle due to protonation.

Esterification of carboxyl groups with acidic methanol or propylene oxide reduced Cd^{2+} binding by 80%, demonstrating that Cd^{2+} binds to carboxyl groups. Blocking amine and hydroxyl groups by formaldehyde reduced binding by 30–50% compared with native and protonated peels, demonstrating that these groups contribute to metal binding.

FTIR spectra of GFPs before and after cadmium binding showed that the carboxylate peak shifted from 1,638 to 1,625 cm^{-1}, confirming the involvement of carboxyl groups. The hydroxyl peak shifted from 3,431 to 3,424 cm^{-1}, indicating involvement of those groups in metal binding.

Overall, it can be concluded that GFPs are a promising biosorbent with high sorption capacity and stability. Cadmium is bound mainly by carboxyl groups with a 1:2 stoichiometry, with some contribution of amine and/or hydroxyl groups.

Acknowledgments

This research was supported by National Research Initiative of the USDA Cooperative State Research, Education, and Extension Service, grant number 2005-35504-16092. A Fulbright grant supporting Dr. M. Iqbal is gratefully acknowledged. Grapefruit by-products were provided courtesy of Peace River Citrus Products, Arcadia, FL.

References

[1] U. Foerstner, G.T.W. Wittmann, Metal Pollution in the Aquatic Environment, Springer, Berlin, 1983.
[2] M.-N. Croteau, S.N. Luoma, A.R. Stewart, Trophic transfer of metals along freshwater food webs: Evidence of cadmium biomagnification in nature, Limnol. Oceanogr. 50 (2005) 1511–1519.
[3] S. McEldowney, D.J. Hardman, S. Waite. Pollution: Ecology and Biotreatment, Longman Scientific and Technical, Harlow, 1993.
[4] J.O. Niragu, J.B. Sprague, Cadmium in the Aquatic Environment, Wiley-Interscience, New York, NY, 1987.
[5] L.D. Benefield, J.A. Morgan, Chemical Precipitation, in: F.W. Pontius Chapter 10 in AWWA Water Quality and Treatment, 4th ed., McGraw-Hill, New York, 1990.
[6] B. Volesky, S. Schiewer, Biosorption of metals, In: M.C. Flickinger, S.W. Drew (Eds), Encyclopedia of Bioprocess Engineering, Wiley, New York, NY, 1999, pp. 433–453.
[7] A. Bhatnagar, A.K. Minocha, M. Sillanpää, Adsorptive removal of cobalt from aqueous solution by utilizing lemon peel as biosorbent, Biochem. Eng. J. 48 (2010) 181–186.
[8] V. Lugo-Lugo, C. Barrera-Díaz, F. Ureña-Núñez, B. Bilyeu, I. Linares-Hernández, Biosorption of Cr(III) and Fe(III) in single and binary systems onto pretreated orange peel, J. Environ. Manage. 112 (2012) 120–127.
[9] M.I. Khaskheli, S.Q. Memon, A.N. Siyal, M.Y. Khuhawar, Use of orange peel waste for Arsenic remediation of drinking water, Waste Biomass Valoriz. 2 (2011) 423–433.
[10] S. Schiewer, M. Iqbal, The role of pectin in Cd binding by orange peel biosorbents: A comparison of peels, depectinated peels and pectic acid, J. Hazard. Mater. 177 (2010) 899–907.
[11] N. Feng, X. Guo, S. Liang, Adsorption study of copper (II) by chemically modified orange peel, J. Hazard. Mater. 164 (2009) 1286–1292.
[12] Z. Xuan, Y. Tang, X. Li, Y. Liu, F. Luo, Study on the equilibrium, kinetics and isotherm of biosorption of lead ions onto pretreated chemically modified orange peel, Biochem. Eng. J. 31 (2006) 160–164.

[13] X. Li, Y. Tang, Z. Xuan, Y. Liu, F. Luo, Study on the preparation of orange peel cellulose adsorbents and biosorption of Cd^{2+} from aqueous solution, Sep. Purif. Technol. 55 (2007) 69–75.
[14] Y. Pei, J. Liu, Adsorption of Pb^{2+} in wastewater using adsorbent derived from Grapefruit peel, Adv. Mater. Res. 391–392 (2012) 968–972.
[15] F.A. Pavan, I.S. Lima, E.C. Lima, C. Airoldi, Y. Gushikem, Use of Ponkan mandarin peels as biosorbent for toxic metals uptake from aqueous solutions, J. Hazard. Mater. 137 (2006) 527–533.
[16] S.V. Ting, E.J. Deszyck, The carbohydrates in the peel of oranges and grapefruit, J. Food Sci. 26 (1961) 146–152.
[17] M.R. Wilkins, W.W. Widmer, K. Grohmann, R.G. Cameron, Hydrolysis of grapefruit peel waste with cellulose an pectinase enzymes, Bioresour. Technol. 98 (2007) 1596–1601.
[18] S. Schiewer, S.B. Patil, Pectin-rich fruit wastes as biosorbents for heavy metal removal: Equilibrium and kinetics, Bioresour. Technol. 99 (2008) 1896–1903.
[19] J.L. Gardea-Torresdey, M.K. Becker-Hapak, J.M. Hosea, D.W. Darnall, Effect of chemical modification of algal carboxylic groups on metal ion binding, Environ. Sci. Technol. 24 (1990) 1372–1378.
[20] K. Chojnacka, A. Chojnacki, H. Goreck, Biosorption of Cr^{3+}, Cd^{2+}, and Cu^{2+} ions by blue-green algae *Spirulina* sp.: Kinetics, equilibrium and the mechanism of the process, Chemosphere 59 (2005) 75–84.
[21] E. Fourest, B. Volesky, Contribution of sulfonate groups and alginate to heavy metal biosorption by the dry biomass of *Sargassum fluitans*, Environ. Sci. Technol. 30 (1996) 277–282.
[22] Y.S. Yun, D. Park, B. Volesky, Biosorption of trivalent chromium on the brown seaweed biomass, Environ. Sci. Technol. 35 (2001) 4353–4358.
[23] R. Ashkenazy, L. Gottlieb, S. Yannai, Characterization of acetone-washed yeast biomass functional groups involved in lead biosorption, Biotechnol. Bioeng. 55 (1997) 1–10.
[24] A. Kapoor, T. Viraraghavan, Heavy metal biosorption sites in *Aspergillus niger*, Bioresour. Technol. 61 (1997) 221–227.
[25] S. Schiewer, B. Volesky, Modeling of the proton-metal ion exchange in biosorption, Environ. Sci. Technol. 29 (1995) 3049–3058.
[26] S. Schiewer, B. Volesky, Ionic strength and electrostatic effects in biosorption of protons, Environ. Sci. Technol. 31 (1997) 1863–1871.
[27] A. Balaria, S. Schiewer, Assessment of biosorption mechanism for Pb binding by Citrus Pectin, Sep. Purif. Technol. 63 (2008) 577–581.
[28] E. Njikam, S. Schiewer, Optimization and kinetic modeling for cadmium desorption from citrus peels: A process for biosorbent regeneration, J. Hazard. Mater. 213–214 (2012) 242–248.
[29] F. Bux, F.M. Swalaha, H.C. Kasan, Assessment of acids as desorbents of metal-ions bound to sludge surfaces, Water SA 21(4) (1995) 319–324.
[30] AOAC Official Methods of Analysis of AOAC International, 18th ed., AOAC International, Gaithersburg, MD, 2005.
[31] W.B. Sinclair, Composition of peel, rag and seeds, In: The Grapefruit, University of California Press, Berkeley, CA, 1972, p. 502.
[32] J. Buffle, Complexation of Reactions in Aquatic Systems—An Analytical Approach, Ellis Horward, Chichester, 1988.
[33] S. Schiewer, M.H. Wong, Metal binding stoichiometry and isotherm choice in biosorption, Environ. Sci. Technol. 33 (1999) 3821–3828.
[34] P. Lodeiro, R. Herrero, M.E.S. de Vicente, Thermodynamic and kinetic aspects on the biosorption of cadmium by low cost materials: A review, Environ. Chem. 3 (2006) 400–418.
[35] S. Bailey, T. Olin, M. Bricka, D. Adrian, A review of potentially low-cost sorbents for heavy metals, Water Res. 33 (1999) 2469–2479.
[36] C. Jeon, J.Y. Park, Y.G. Yoo, Biosorption model for binary adsorption sites, J. Microbiol. Biotechnol. 11 (2001) 781–787.
[37] Y. Murphy, H. Hughes, P. McLoughlin, Cu(II) binding by dried biomass of red, green and brown macroalgae, Water Res. 41 (2007) 731–740.
[38] S.H. Min, J.S. Han, E.W. Shin, J.K. Park, Improvement of cadmium ion removal by base treatment of juniper fiber, Water Res. 38 (2004) 1289–1295.
[39] I. Villaescusa, N. Fiol, M. Martinez, N. Miralles, J. Poch, J. Serarols, Removal of copper and nickel ions from aqueous solutions by grape stalk wastes, Water Res. 38 (2004) 992–1002.
[40] R.P. De Carvalho, J.R. Freitas, A.M.G. de Sousa, R.L. Moreira, M.V.B. Pinheiro, K. Krambrock, Biosorption of copper ions by dried leaves: Chemical bonds and site symmetry, Hydrometallurgy 71 (2003) 277–283.